16. Isagi, Y., Kawahara, T., Kamo, K. and Ito, H., *Plant Ecol*., 1997, **130**, 41–52.
17. Edenhofer, O. *et al.*, In *Climate Change 2014: Mitigation of Climate Change. Contribution of Working Group III to the Fifth Assessment Report of the Intergovernmental Panel on Climate Change*, Cambridge University Press, Cambridge, UK, 2014.
18. Singh, A. N. and Singh, J. S., *For. Ecol. Manage.*, 1999, **119**, 195–207.
19. Uchimura, E., *Bull. For. Prod. Res. Inst*., 1978, **301**, 79–118.
20. Suzuki, T., *Rep. Trop. Agric. Res. Cent*., 1989, **65**, 94–97.
21. Isagi, Y., Kawahara, T. and Kamo, K., *Ecol. Res*., 1993, **8**, 123–133.
22. Singh, K. A. and Kochhar, S. K., *J. Bamboo Rattan*, 2005, **4**, 323–334.
23. Shanmughavel, P. and Francis, K., *Biomass Bioenerg.*, 1996, **10**, 383–391.
24. Kumar, B. M., Rajesh, G. and Sudheesh, K. G., *J. Trop. Agric*., 2005. **43**, 51–56.
25. Embaye, K., Weih, M., Ledin, S. and Christersson, L., *For. Ecol. Manage.*, 2005, **204**, 159–169.
26. Castañeda-Mendoza, A., Vargas-Hernández, J. J., Gómez-Guerrero, A., Valdez-Hernández, J. I. and Vaquera-Huerta, H., *Agrociencia*, 2005, **39**, 107–116.
27. Quiroga, R., Ricardo, A., Tracey, Li., Gonzalo, L. and Andersen, L. E., Development Research Working Paper Series No. 04/2013, 2013.
28. Thockhom, A. and Yadava, P. S., *Trop. Ecol.*, 2017, **58**, 23–32.

Received 14 June 2018; revised accepted 13 March 2019

MUKTA CHANDRA DAS*
ARUN JYOTI NATH
ASHESH KUMAR DAS

Department of Ecology and Environmental Science,
Assam University,
Silchar 788 011, India
**For correspondence.*
e-mail: dasmukta04@gmail.com

28 August 2018 (M_w 4.5) Bengal Basin earthquake highlights active basement fault beneath the sediments

The India Meteorological Department (IMD) reported an earthquake of magnitude 4.8 at IST 18 h 33 min and 29 sec on 28 August 2018. The epicentre of the earthquake was located in the Bengal Basin (lat. 22.6°N, long. 87.7°E) at a distance of ~67 km west of the city of Kolkata (Figure 1). Strong to moderate ground shaking was felt in the epicentral zone and in surrounding districts of East Midnapore, West Midnapore, Jhargram and Bankura. Given the moderate size of the event, there was neither loss of life nor cases of injury due to the earthquake. However, some buildings close to the epicentral region, developed cracks from the shaking. Albeit the moderate size of the earthquake, we consider this to be a significant one given its location in the intra-plate region of the Bengal Basin. The epicentre of the earthquake is located between the mapped Pingla Fault, to its west, and the Garhmayna Khanda Ghosh Fault, to its east[1,2]. Farther east the Eocene Hinge Zone marks the paleo continent-ocean boundary of the eastern margin of India, and transit northeastward into the active Dawki Fault, along the southern margin of the Shillong Plateau[3]. These faults form an en-echelon pattern of passive continental margin growth faults and remain buried below the sediment cover[4]. However, changes in the stress patterns within the continental interior and flexural loading of the sediments along the basin margin can

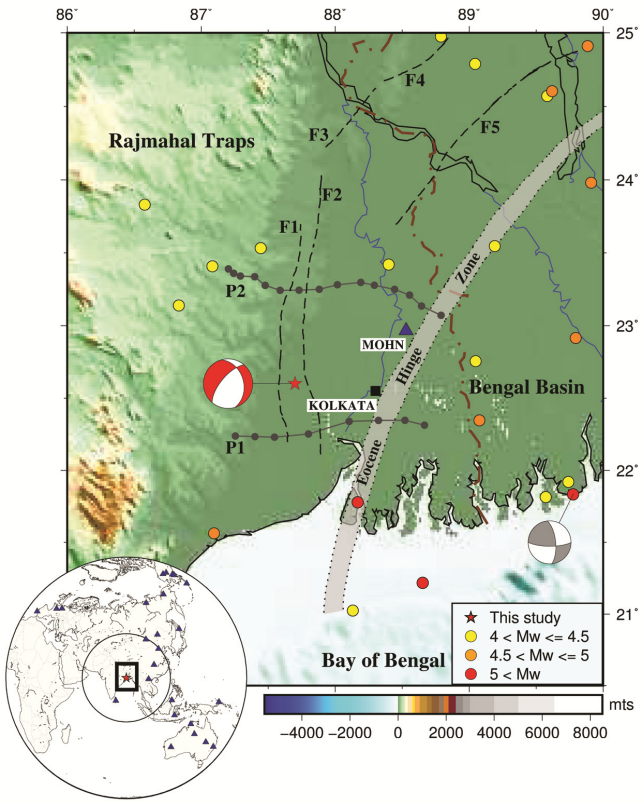

Figure 1. Topographic map of the Bengal Basin (boxed in the inset map) with plot of the 28 August 2018 M_w 4.5 earthquake epicentre (red star) taken from IMD and the source mechanism computed in this study (red focal sphere). Previous earthquakes in this region (from ISC reviewed catalogue) are plotted as circles (colour coded by magnitude) and the mechanism (from Global CMT catalogue) plotted as grey focal sphere. Sub-surface faults are plotted as dashed black lines and labelled F1, Pingla Fault; F2, Garhmayna Khanda Ghosh Fault; F3, Jangipur Fault; F4, Gaibandha Fault; F5, Debagram Bogra Fault[18]. The two Deep Seismic Sounding (DSS) profiles are labelled as P1 and P2 (refs 1, 2). Inset map plots the GDSN stations (blue triangles) from which data has been used for the source mechanism computation (Figure 3).

reactivate these faults, resulting in significant seismic hazard to nearby regions. Occasional light-to-moderate intra-plate earthquakes have occurred in the past, beneath this region of the western Bengal Basin (Figure 1).

In this study we use: (a) broadband waveform data recorded by the Indian Institute of Science Education and Research Kolkata (IISER-K) Seismological Observatory (MOHN – 22.96°N, 88.53°E), to compute the fault rupture parameters of the earthquake (Figure 2); (b) teleseismic data obtained from the Global Digital Seismic Network (GDSN) stations, in the epicentral distance range of 30°–80°, to model the source mechanism. Finally, we discuss our results in the context of the seismotectonics of the Bengal Basin.

We pick the *P*-wave and *S*-wave arrival times from the vertical and transverse component seismograms respectively, recorded at the MOHN observatory (Figure 2). The $t_s - t_p$ time is calculated to be ~13 sec. Using the receiver function derived velocity model[5] we compute the hypocentral distance for the earthquake to be ~85 km. Time–distance computation of direct and Moho refracted phases, for a ~40 km thick crust with a mantle half-space, reveals that the first arriving body waves are the direct P_g and S_g phases. We use the S_g phase to compute fault rupture parameters (e.g. seismic moment, moment magnitude, fault rupture area and stress drop) of the earthquake.

For a symmetric rupture model[6], the *S*-wave displacement spectrum is a function of the scalar seismic moment (M_0), corner frequency (f_0), average crustal *S*-wave velocity (β), source rock density (*rho*), geometrical spreading ($1/R$) and the quality factor (Q) of the crust[7]. The recorded waveform is corrected for instrument response and converted to ground velocity. The ground velocity waveforms are integrated to obtain ground displacement in metres. The *S*-waveform is windowed on the transverse component (Figure 2 *a*) and fast Fourier transformed to obtain the frequency spectrum at the station. The effects of geometrical spreading are removed using a $1/R$ model for body waves, and the spectrum is corrected for seismic attenuation using a frequency dependent relationship $Q(f) = Q_0 f^{\eta}$. We use Q_0 of 300 and η of 0.9 for the Bengal Basin[8]. The corrected *S*-wave source spectrum (Ω_0) is fitted using a theoretical spectrum of $\Omega_0/(1 + (f/f_0)^2)$; where f_0 is the corner frequency (Figure 2 *b*). To obtain the best fitting spectrum, we implement a random search algorithm to explore over a range of spectral amplitudes (Ω_0) and corner frequencies (f_0). The best-fitting spectrum is obtained by minimizing the misfit between the observed and theoretical spectra in a least-squares sense. The best fitting value of Ω_0 is used to compute the scalar seismic moment (M_0), found to be 6.03×10^{15} N-m, and yields a moment magnitude (M_w) of 4.45. The corresponding f_0 value is used to estimate the circular fault radius (a) (ref. 9), which is computed to be ~4 km^2. The scalar seismic moment (M_0) and the fault radius (a) is used to calculate the stress drop[7], which is found to be ~19 bars.

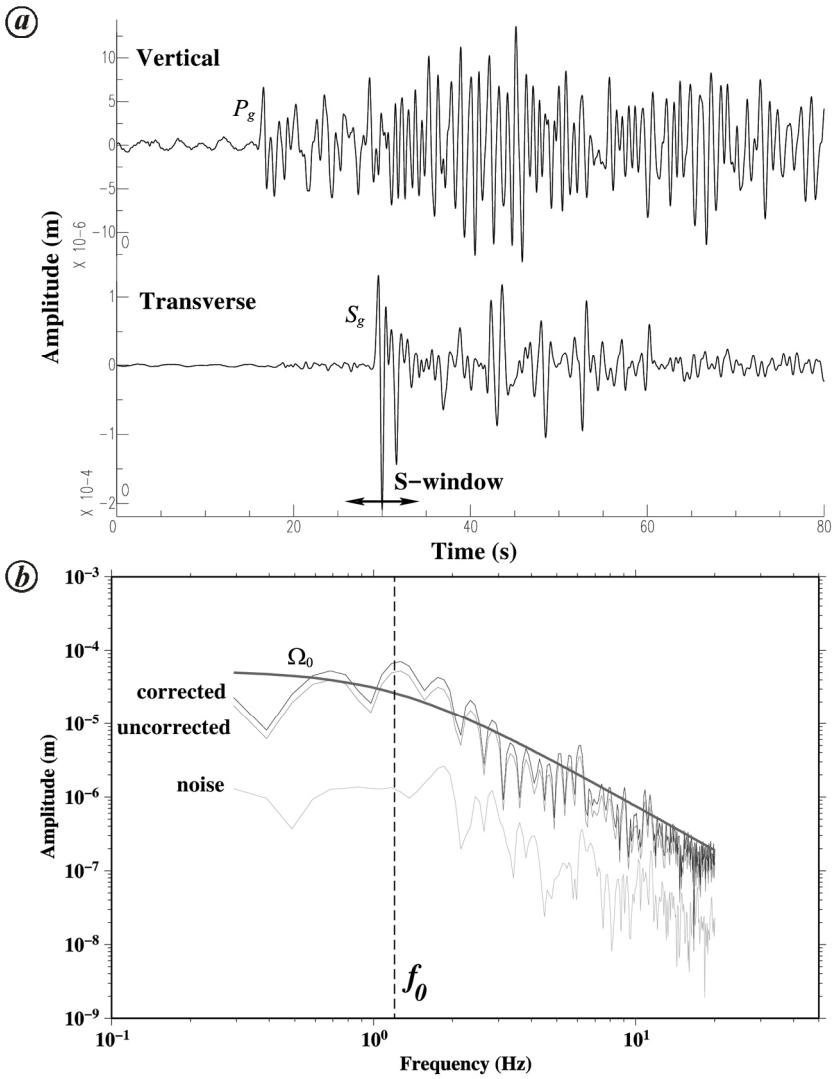

Figure 2. ***a***, Plot of vertical and transverse velocity waveforms recorded by the IISER-K Seismological Observatory (MOHN), bandpass filtered between 1 and 100 s. The first arriving body waves are P_g and S_g marked on the vertical and transverse waveforms respectively. The *S*-wave window used for computing the source spectrum is marked on the transverse component. ***b***, Plot of *S*-wave spectrum at the station (labelled uncorrected), corrected for geometrical spreading and attenuation (labelled corrected) and for pre-signal noise. The best fitting curve with Ω_0 and f_0 is shown in the figure.

We use teleseismic body waveforms from 27 Global Digital Seismic Network (GDSN) stations (Figure 1) to model the source mechanism of the earthquake using waveform inversion technique. The broadband data is deconvolved from the instrument response and reconvolved with a long-period WWSSN instrument filter of 15–100 sec. *P*- and *SH*-waveforms windowed from the vertical and tangential components respectively, are used for the analysis. We use the moment

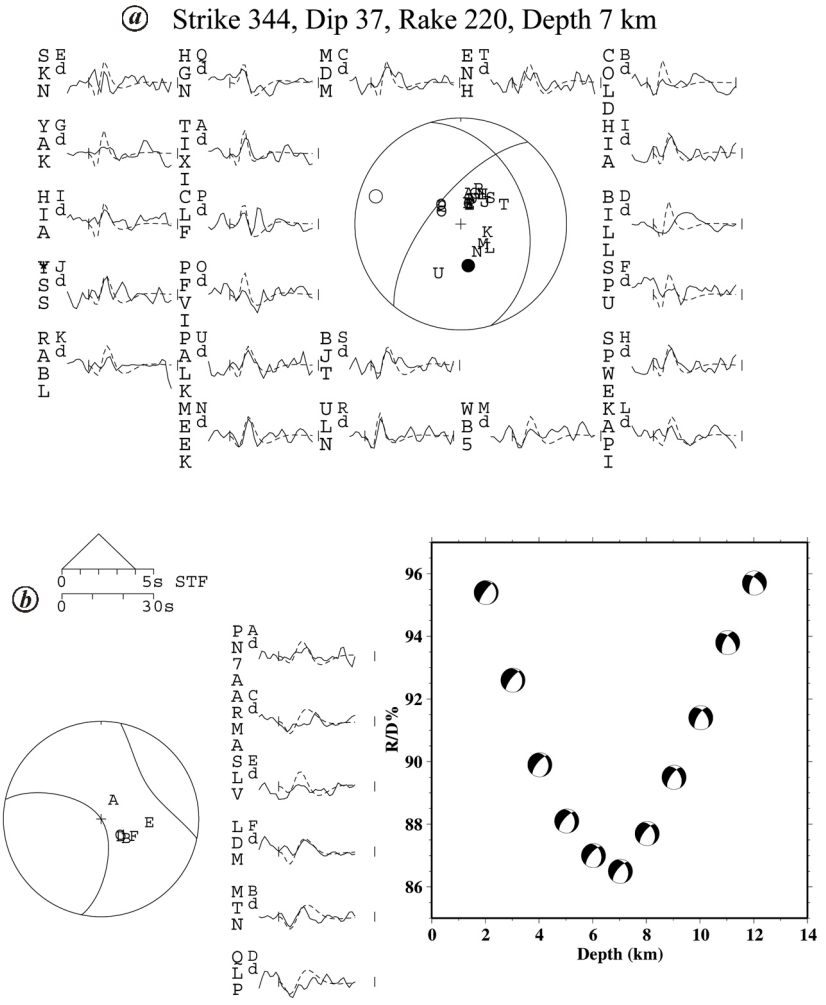

Figure 3. ***a***, P (top) and ***b***, SH (bottom) focal mechanism and waveforms (observed – bold, synthetic – dashed) for our minimum-misfit solution. The station code for each waveform is accompanied by a letter corresponding to its position in the focal sphere. The time window used for the inversion is marked by vertical lines on each waveform. The pressure and tension axes are plotted as solid and open circles on the *P*-wave focal sphere. ***c***, Hypocentral depth test for the minimum misfit source mechanism solution.

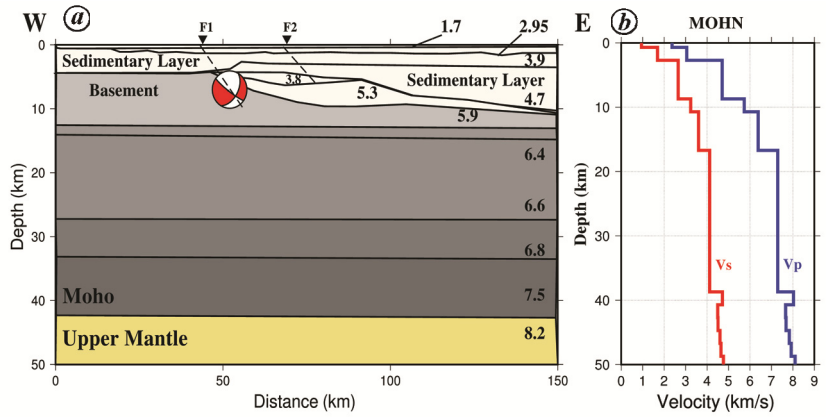

Figure 4. ***a***, West–East crustal cross-section along DSS profile P1 (Figure 1) with overlay plot of the focal mechanism. The numbers represent *P*-wave velocity in km/s from the DSS profile. Outcrop and sub-surface disposition of the Pingla (F1) and Garhmayna Khanda Ghosh (F2) faults show that the earthquake originated on the Pingla Fault. ***b***, The velocity model for the station Mohanpur (MOHN) used for computing the *P* and *S*-wave arrival times and the source mechanism of the earthquake. Note the remarkable similarity of the velocity models from the DSS profile and the MOHN station obtained from receiver function inversion.

tensor inversion algorithm of McCaffrey and Abers[10] to estimate the geometry of the fault plane (strike and dip), rake of the slip vector, and the focal depth of the earthquake. The algorithm minimizes the least squares misfit between the observed and synthetic *P*- and *SH*-waveforms using an iterative approach. Details of the algorithm are available in Nabelek[11] and McCaffrey and Nabelek[12] and the methodology has been discussed in detail in previous studies[13,14]. The best fitting solution for the earthquake has one of the nodal planes with strike of ~344°, dip of ~37°, rake of ~220° and a focal depth of ~7 km (Figure 3). However, from this analysis of far field waveform fit, it is not possible to distinguish the fault plane from the auxiliary plane. This is discussed in the next section by putting the solution in context of the regional geology. The uncertainties associated with the best fitting solution have been obtained by fixing one parameter at a time and running the inversion. The best estimates for the depth uncertainty is ±3 km (Figure 3 *c*) and for the strike, dip and rake are ±10°.

We compare the hypocentral location and source mechanism of the moderate (M_w ~ 4.5) Bengal Basin earthquake with the sub-surface structure from Deep Seismic Sounding (DSS) profiles[1,2] in the Bengal Basin (Figure 4 *a*). We have chosen the cross-section along profile P1 (Figure 1) as the earthquake epicentre lies in close proximity of this profile. It is observed that the epicentre of the earthquake lies between the Pingla Fault (west) and the Garhmayna Khanda Ghosh Fault (east). Both these faults are known to be part of the series of en-echelon east dipping basin margin faults, almost parallel to the Eocene Hinge Zone, which marked the paleo continent-ocean boundary of the Indian eastern margin[3,15]. The sub-surface model from the DSS profile closely matches the receiver function derived *S*-wave velocity model beneath the MOHN station (Figure 4 *b*). Given the ~7 km focal depth of the earthquake, we infer that it originated on the east dipping Pingla Fault (Figure 4 *a*). Either nodal planes could be the fault plane, but the similarity in orientation of the NNW–SSE striking nodal plane with the Pingla Fault, suggest this to be the fault plane of this earthquake. We therefore infer that the earthquake faulting occurred on a dextral oblique slip normal fault with the pressure axis

oriented in the N–S direction. Comparison of the hypocentral location and geometry of this fault plane with the subsurface structure from the DSS profile shows that the earthquake ruptured a segment of the Precambrian gneissic basement fault in contact with the eastward thickening sedimentary layer (Figure 4 *a*). We further speculate that this event possibly reactivated the pre-existing basement structure in response to the combined effect of the intra-plate stresses from the N20°E motion of India plate and the E–W flexure of the basement due to sediment loading in the Bengal Basin. Although this event was of moderate size, reactivation of basement faults has the potential to cause moderate-to-large earthquakes, and should be accounted for while quantifying seismic hazard for the region.

The moderate earthquake which occurred in the western Bengal Basin on 28 August 2018 highlights active fault beneath the thick sedimentary cover of the Bengal Basin. The epicenter of the earthquake was reported to be ~67 km west of Kolkata, by the IMD. We use local waveform data recorded at the IISER Kolkata Seismological Observatory to model the source parameters; and teleseismic data from the Global Digital Seismic Network (GDSN) stations to model the focal mechanism of the earthquake. Fitting the *S*-wave source spectra we obtain seismic moment (i.e. energy release) of 6.03×10^{15} N-m and moment magnitude (M_w) of 4.45. The earthquake ruptured ~4 km^2 fault area and had a stress drop of ~19 bars. Moment tensor inversion of teleseismic data reveals an oblique slip normal fault earthquake with a hypocentral depth of 7 ± 3 km. We compare the source mechanism with mapped faults in the region and interpret that the earthquake occurred on the E–NE dipping Pingla Fault (strike ~344° and dip ~37°) with a dextral strike–slip motion. This fault is among the mapped en-echelon basement faults at the junction of the Precambrian gneissic basement and the overlying Bengal Basin sediments, and is skirted by the Eocene Hinge Zone to its east. We conjecture that the earthquake occurred in response to intra-plate stresses due to the N20°E motion of the Indian plate, and the E–W flexure of the basement due to sediment loading in the Bengal Basin.

1. Kaila, K. L., Reddy, P. R., Mall, D. M., Venkateswarul, N., Krishna, V. G. and Prasad, A. S. S. S. R. S., *Geophys. J. Int.*, 1992, **111**(1), 45–66.
2. Kaila, K. L. *et al.*, *Geophys. J. Int.*, 1996, **124**, 175–188.
3. Mitra, S., Priestley, K. F., Borah, K. J. and Gaur, V. K., *J. Geophys. Res.: Solid Earth*, pages n/a–n/a, 2018; ISSN 2169-9356. doi: 10.1002/2017JB014714. URL http://dx.doi.org/10.1002/2017JB014714.2017JB014714.
4. Alam, M., Alam, M. M., Curray, J., Chowdhury, M. L. R. and Gani, M. R., *Sediment. Geol.*, 2003, **155**, 179–208.
5. Bohidar, S., Crustal structure beneath western Bengal Basin, Master's thesis, Indian Institute of Science Education and Research Kolkata, 2018.
6. Brune, J. N., *J. Geophys. Res.*, 1970, **75**, 4997–5009.
7. Havskov, J. and Ottemoller, L., *Routine Data Processing in Earthquake Seismology: With Sample Data, Exercises and Software*, Springer, 2010.
8. Sharma, S. and Mitra, S., In 20th EGU General Assembly, EGU2018, Proceedings from the conference held 4–13 April 2018 in Vienna, Austria, EGU General Assembly, 2018, p. 1148.
9. Madariaga, R., *Bull. Seismol. Soc. Am.*, 1976, **66**, 639–666.
10. McCaffrey, R. and Abers, J., SYN3: A program for inversion of teleseismic body wave form on microcomputers. Technical Report AFGL-TR-0099, Air Force Geophysical Laboratory, Hanscomb Air Force Base, Massachussets, 1988.
11. Nabelek, J., Determination of earthquake source parameters from inversion of body waves. Ph D thesis, Massachusetts Institute of Technology, 1984.
12. McCaffrey, R. and Nabelek, F., *J. Geophys. Res.*, 1987, **92**, 441–460.
13. Mitra, S., Wanchoo, S. and Priestley, K. F., *Bull. Seismol. Soc. Am.*, 2014, **104**(2), 1013–1019; doi:10.1785/0120130216.
14. Himangshu Paul, Mitra, S., Bhattacharya, S. N. and Suresh, G., *Geophys. J. Int.*, 2015, **201**(2), 1070–1081.
15. Supriya Sengupta, *Am. Assoc. Pet. Geol. Bull.*, 1966, **50**(5), 1001–1017.
16. Goldstein, P., Dodge, D., Firpo, M. and Minner, L., In *The IASPEI International Handbook of Earthquake and Engineering Seismology* (eds Lee, W. H. K. *et al.*), Academic Press, London, 2003.
17. Wessel, P. and Smith, W. H. F., *EOS Trans. AGU*, 1998, **79**, 579.
18. Dasgupta, S. *et al.*, *Seismotectonic Atlas of India and its Environs*, Geological Survey of India, Kolkata, 2000.

ACKNOWLEDGEMENTS. Seismograms used for source mechanism study have been downloaded from Incorporated Research Institutions in Seismology (IRIS) Data Management Center (DMC) (www.iris.edu/dms/dmc/). Data preprocessing and part of the analysis was performed using Seismic Analysis Code 2000, version 100 (ref. 16). All plots were made using the Generic Mapping Tools version 4.0 (www.soest.hawaii.edu/gmt; Wessel and Smith[17]). S.D., D.P. acknowledge IISER Kolkata for Ph D fellowship, J.C. acknowledges UGC-SRF, M.G. acknowledges CSIR-JRF, J.K. acknowledges DST-SERB NPDF and S.M. acknowledges ARF support from IISER Kolkata.

Received 2 September 2018; revised accepted 6 March 2019

SIDDHARTH DEY
DEBARCHAN POWALI
JASHODHARA CHAUDHURY
MONUMOY GHOSH
RIDDHI MANDAL
JYOTIMA KANAUJIA
SUPRIYO MITRA*

Department of Earth Sciences,
Indian Institute of Science Education and Research Kolkata,
Mohanpur 741 246, India
**For correspondence.*
e-mail: supriyomitra@iiserkol.ac.in